EUCAS2023, LP-HF1-12S, T. Mato, R. Inoue, H. Ueda, S.B. Kim, and S. Noguchi,

Turn-to-Turn Contact Resistance Measurement of NI REBCO Double Pancake Coils

Takanobu Mato, Ryota Inoue, Hiroshi Ueda, SeokBeom Kim, and So Noguchi, *Member, IEEE*

***Abstract*—The turn-to-turn contact resistance/resistivity is one of the most important parameters for no-insulation (NI) rare-earth barium copper oxide (REBCO) pancake coils. Our group has been working on the measurement of the contact resistances of NI REBCO pancake coils by alternating current, called a low-frequency AC current (LFAC) method. One of the advantages is that the LFAC method is able to measure the field and current dependencies on contact resistances in principle, while the conventional discharge method is not. The effectiveness of the LFAC method was well demonstrated using a single pancake coil.**

In this paper, contact resistances of a double pancake coil were measured with the LFAC method although the upper and lower pancake coils had different turn-to-turn contact conditions due to an accident. The experiment results well agree with the simulation results. In addition, the contact resistances of each pancake coil can be separately specified. The contact resistances measured with a conventional sudden discharge method also have a good agreement with the LFAC method; however, the contact resistance of sudden discharge simulation is underestimated. Meanwhile, the energy consumptions are also complicated. We need further investigation for multi-stacked NI pancake coils in the near future.

***Index Terms*—no-insulation, REBCO, turn-to-turn contact resistance, LFAC method, AC current.**

I. Introduction

In 2011, Hahn et al. proposed the no-insulation (NI) winding technology applied for a high-temperature superconducting (HTS) pancake coil [1]. Thereafter, many NI rare-earth barium copper oxide (REBCO) pancake coils have shown great performances, *e.g.* high thermal stability, due to an extra current sharing a path through turn-to-turn contact surfaces and high tolerance against local critical-current (I_c) degradations [2]-[8]. The most fundamental parameter of NI REBCO pancake coils is a turn-to-turn contact resistance, often called the characteristic resistance. The turn-to-turn contact resistances largely affect the current behaviors such as field delay and thermal stability. Hence, the measuring technique of turn-to-turn contact resistance is practically required.

The sudden discharge method [9] is used in most of the research related to the NI technique to measure the turn-to-turn contact resistances. In the contact resistance measurement, a power source ramps up to an arbitrary current, and then it is suddenly cut off the coils; consequently, the coil current as well as the magnetic field decays exponentially. The contact resistance is obtained by dividing the time constant by the coil inductance. The sudden discharge method is simple and well-established.

Our group has been studying another method using low-frequency AC current (LFAC) [10]. In the LFAC method, an AC current at a relatively low frequency is applied to NI REBCO pancake coils, and the contact resistance is estimated from the coil impedance measured. One advantage is that the LFAC method can measure the current dependence on the contact resistances [11]. The previous studies have shown the validity of the LFAC method under several conditions [12]-[14], and a detailed simulation was also conducted [15]; nevertheless, the target is only single pancake coils. It is, therefore, necessary to measure the contact resistance of double pancake (DP) coils as an advanced step.

We prepared an NI REBCO DP coil with a winding tension of 1 kgf to apply the LFAC method. However, it turned out that the winding tension of the upper pancake coil was accidentally loosened, thus the DP coil with different winding tensions between the upper and lower coils was tested in this paper. The contact resistances were estimated with the LFAC method, and the results were discussed together with the simulation using a partial equivalent element circuit (PEEC) model [16]. The LFAC results were also compared with that of the sudden discharge method.

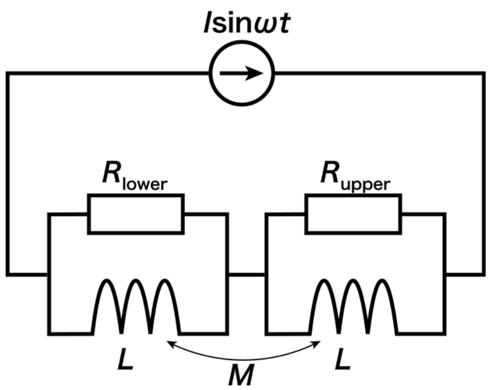

Fig. 1. Electrically equivalent circuit of NI REBCO DP coil.

Manuscript received. This work was supported by the JSPS KAKENHI under Grant No. 22KJ0104. (Corresponding author: Takanobu Mato.)

T. Mato and S. Noguchi were with Graduate School of Information Science and Technology, Hokkaido University, Sapporo, 060-0814 Japan (e-mail: e-mail: mato@em.ist.hokudai.ac.jp, noguchi@ssi.ist.hokudai.ac.jp).

R. Inoue, H. Ueda, and S.B. Kim were with Faculty of Environmental, Life, Natural Science and Technology, Okayama University, Okayama, 700-0082 Japan

Color versions of one or more of the figures in this article are available online at http://ieeexplore.ieee.org

Digital Object Identifier will be inserted here upon acceptance.

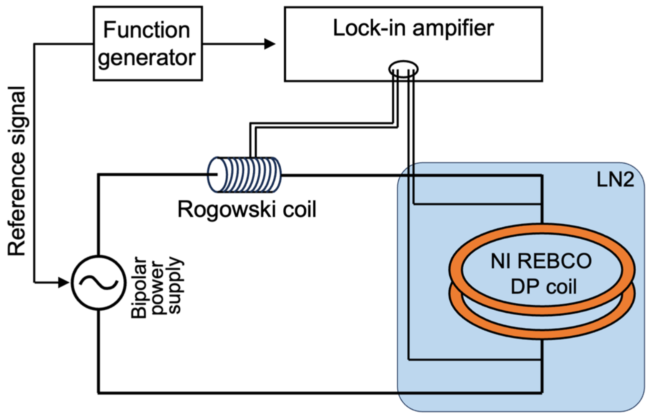

Fig. 2. Schematic image of LFAC measurement setup.

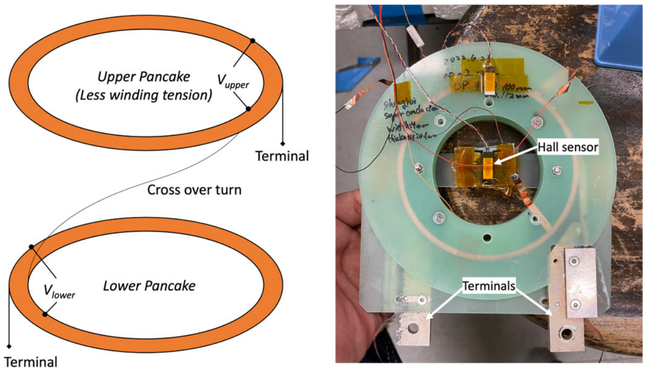

Fig. 3. Measured NI REBCO DP coil and arrangement of voltage taps.

II. LFAC Method and Experiment Setups

Fig. 1 shows an electrically equivalent circuit of an NI REBCO DP coil with different turn-to-turn contact resistances R_{upper} and R_{lower} when an operating current carries below a critical current. Each pancake coil theoretically has the same inductance L, coupled with a mutual inductance M. In the LFAC method, a sinusoidal current $\dot{I}$ at an appropriate angular frequency ω (low frequency) which satisfies the following relation is applied to an NI DP coil:

$$j\omega L \gg R_{\mathrm{upper}} \text{ and } R_{\mathrm{lower}}. \quad (1)$$

Under the condition, the impedances of the NI DP coil and each pancake coil theoretically become:

$$\dot{Z}_{\mathrm{all}} = R_{\mathrm{all}} \quad (2)$$

$$\dot{Z}_{\mathrm{upper}} = R_{\mathrm{upper}} \quad (3)$$

$$\dot{Z}_{\mathrm{lower}} = R_{\mathrm{lower}}, \quad (4)$$

where R_{all} is the resistance of the NI DP coil, ideally $R_{\mathrm{upper}} + R_{\mathrm{lower}}$.

Fig. 2 illustrates the experimental setup of the LFAC measurement. The NI REBCO DP coil was connected to a bipolar power supply, and it was cooled with liquid nitrogen. A Rogowski coil was attached to a current lead to measure the current phase. The coil voltages were measured with a lock-in amplifier. The bipolar power supply outputted a sinusoidal current according to the reference signal from the function generator. The reference signal was also sent to the lock-in amplifier to detect phase differences between operating current and coil voltages. Fig. 3 shows the measured NI REBCO DP coil and the arrangement of the voltage taps. Table I lists the specifications of the NI REBCO DP coil. The REBCO tape from Shanghai Superconductor with 4.0 mm width and 0.1 mm thickness was employed. Both the upper and lower coils were wound with a tension of 1 kgf; however, the actual tension of the upper pancake coil is lower than the lower pancake coil due to accidental mishandling.

TABLE I
Tape and Coil Specifications

Parameters	Values
Tape width [mm]	4.0
Tape thickness [mm]	0.1
Inner diameter [mm]	100
Outer diameter [mm]	112
Height [mm]	9.0
Number of turns (each)	60
Coil I_c (upper and lower pancake) [A]	65.5, 65.3
Coil inductance [mH]	2.70

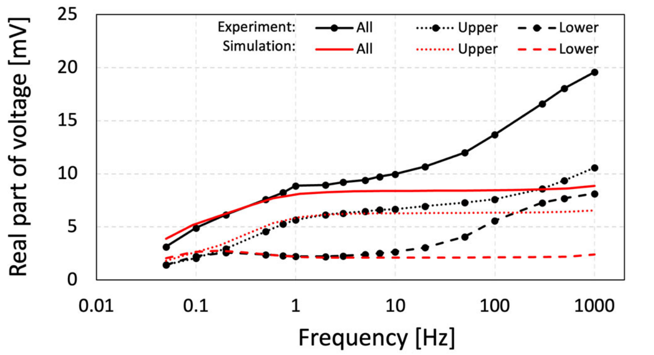

Fig. 4. Real part of voltage. The value divided by current amplitude (10 A) corresponds to equivalent resistance.

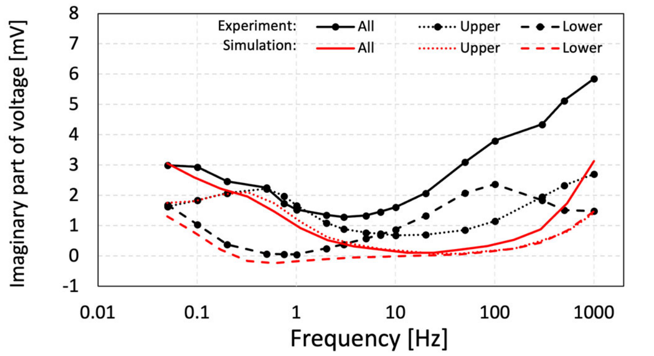

Fig. 5. Imaginary part of voltage.

III. LFAC Measurement Results

A. Experimental results

A sinusoidal current with an amplitude of 10 A was applied to the NI REBCO DP coil. Each pancake coil voltage was measured in the frequency range from 0.05 to 1000 Hz. Figs. 4, 5, and 6 show the real and imaginary parts of the measured voltages and the phase differences between voltage and current, respectively.

The real part of the measured voltage is almost the same as the imaginary part at 0.05 Hz. This means that a large amount of the current flows in the circumferential direction. The inductive voltage appears at a non-negligible level and the contact resistance cannot be estimated at the frequency. Then, with the increase of frequency, the real part of the upper pancake voltage increases up to 1 Hz, whereas the imaginary part of both upper and lower pancake voltages. It is noted that the increase of the imaginary part of the upper pancake (decrease of the lower pancake) at around 0.3 Hz is due to the magnetic coupling between pancakes.

In the middle frequencies (1-10 Hz), the real parts of the pancake voltages are almost constant. Also, the inductive voltages and the phases are sufficiently low. Thus, it is considered that almost all the current flows in the radial direction on both upper and lower pancake coils. The averaged real parts in the region are 9.37 mV in total, 6.31 mV and 2.39 mV for the upper and lower pancakes. Since the alternating current with an amplitude of 10 A is applied, the contact resistances are estimated as 937, 631, and 239 μΩ for all, upper and lower pancakes, respectively.

In the higher-frequency region than 10 Hz, the imaginary voltages increase simply because of the high frequency. Both upper and lower pancake coils exhibit the high real part of the measured voltage. The current would directly flow between the terminals, like a short circuit mode. Since the current flows in a small area of the turn-to-turn contact surfaces, the NI DP coil exhibits high equivalent resistances (real part of the voltages) and high equivalent inductances (imaginary part of the voltages.)

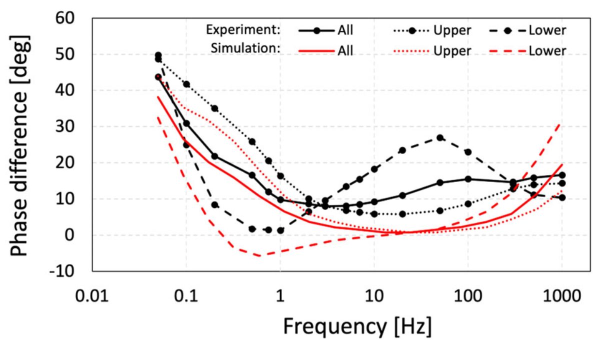

Fig. 6. Phase between applied current and voltages.

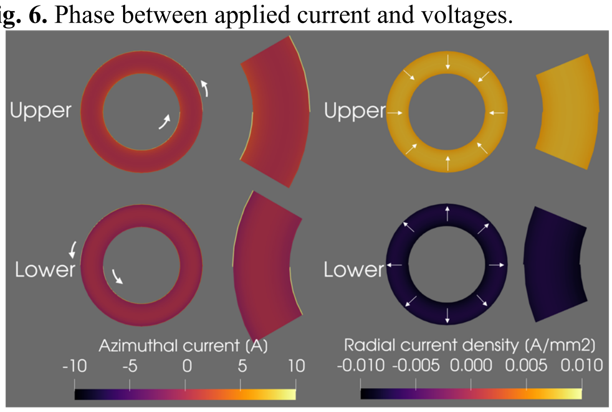

Fig. 7. Current distribution of NI REBCO DP coil when operating current reach its peak. A 1-Hz AC current is applied. The current flows uniformly in a radial direction. The arrows show the directions of the current.

TABLE II
ESTIMATED CONTACT RESISTANCES BY LFAC METHOD

	Experimental	Simulation
DP (all)	937 μΩ	832 μΩ
Upper pancake	631 μΩ	620 μΩ
Lower pancake	239 μΩ	212 μΩ

B. Simulation results

The contact resistances were also estimated, fitted with the 2-D PEEC model on $R-\theta$ plane by changing the contact resistivities of the upper and lower pancake coils. Figs. 4-6 also plot the real and imaginary parts of the simulated voltages and the phase differences between voltage and current. The cross-over turn is not considered in the PEEC model.

The simulation and experimental results well agree in the low- and middle-frequency regions (0.05-10 Hz). In the simulation, the uniform turn-to-turn contact resistivity is assumed in both upper and lower pancake coils: 138 μΩ·cm^2 and 45.8 μΩ·cm^2 for the upper and lower. The contact resistances are estimated using the same procedures as in the experimental results: 620 μΩ and 212 μΩ for the upper and lower pancake coils, separately. The total contact resistance is 832 μΩ.

The estimated turn-to-turn contact resistances are summarized in Table II. The values are consistent among the experiment and simulation. Especially, the contact resistances of upper and lower pancakes agree well. As we expected, the upper pancake coil loosely wound has a contact resistance three times as high as the lower pancake coil. The total contact resistance estimated by the simulation is slightly different from the measurement. It would be caused by the resistance of the cross-over turn. The small resistive voltage corresponding to ~30 μΩ was observed between the upper and lower pancakes in the experiment, although the resistance is not enough to explain the difference.

Fig. 7 shows the peak-current distributions of the NI REBCO DP coil when the 1-Hz AC current is applied. Almost all the current uniformly flows in the radial direction. In the experiment, the current is expected to uniformly flow through turn-to-turn contact resistances; however, it is impossible to make it clear so far.

IV. SUDDEN DISCHARGE RESULTS

A. Experimental and Simulation results

The contact resistances were also evaluated with a conventional sudden discharge method. The operating current was ramped up to 50 A, and then it dropped off to zero. The contact resistances are obtained from the field decay profile. Fig. 8 shows the normalized axial field at the magnet center. The axial field is attenuated exponentially. The time constant τ was estimated as 2.78 s from the measured field waveform. Hence, the turn-to-turn contact resistance of the NI DP coil was specified as 971 μΩ with the relation of $\tau = L/R_{\mathrm{cn}}$ [9]. It well agrees with the contact resistance obtained from the LFAC method.

The dotted red line in Fig. 8 represents the normalized field computed with the PEEC model. Here, the same contact resistivities as in the simulation of the LFAC measurement are used: 138 μΩ·cm^2 and 45.8 μΩ·cm^2 for upper and lower, respectively. The simulated time constant from the simulation is 4.26 s, and the corresponding contact resistance is 633 μΩ with the relation of $\tau = L/R_{\rm cn}$.

The experimental contact resistance conventionally calculated from the time constant shows good agreement with the result of the LFAC method (Table II), while the contact resistance derived from the sudden discharge simulation is underestimated when compared with the LFAC method. The mechanism of the discrepancy needs to be addressed as a future task; however, we currently think there needs phenomena related to the fast-current change mode. In the high-frequency region of LFAC measurement (Fig. 4), the mismatch between the experiment and simulation is significant. The discrepancy was also found in the sudden discharge method, where the coil current changes fast. It is also noted that a similar kind of discrepancy can be found in [17]

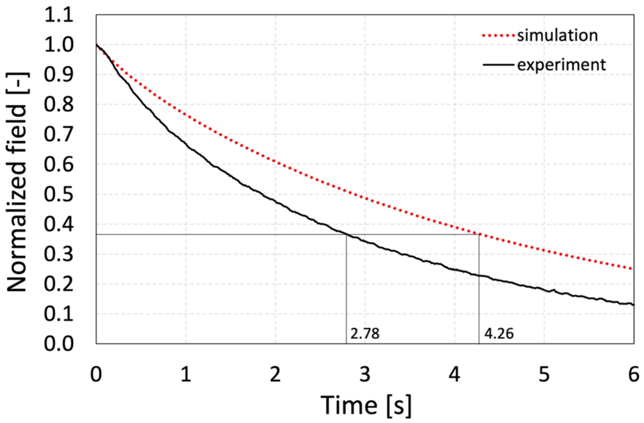

Fig. 8. Field decay and time constants.

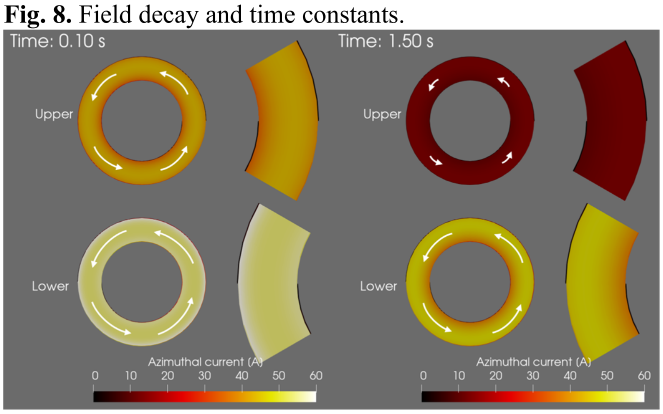

Fig. 9. Current distribution of NI REBCO double pancake coil after sudden discharge at 0.1 s (left) and 1.5 s (right).

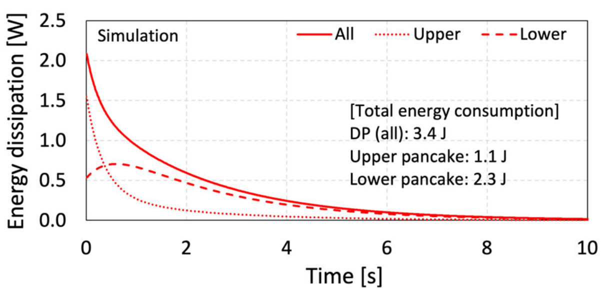

Fig. 10. Energy dissipation on each pancake. Unbalanced energy consumption occurs due to the different contact resistances.

B. possible danger of sudden discharge method

Here, we discuss the stability of the sudden discharge method regarding the large-scale application. It should be mentioned that the sudden discharge itself needs to be cautiously applied to a DP coil with different contact resistances. First, the current beyond the initial current flows in a pancake coil with lower contact resistance than the other. Fig. 9 shows the simulated current distribution during the sudden discharge at 0.1 s and 1.5 s although the underestimated contact resistance is used. At the beginning of the discharge (0.1 s), the current on the upper pancake decays quickly; whereas the current is induced in the lower pancake coils, exceeding the initial current. Second, the energy consumption is unbalanced due to the different contact resistances. Fig. 10 depicts the energy dissipation on each pancake coil during the sudden discharge. The energy consumption on the upper and lower coils is 1.1 J and 2.3 J, respectively. We will further investigate whether unbalanced contact resistances downgrade the thermal stability of NI REBCO pancake coils.

V. Conclusion

In this work, the contact resistances of a no-insulation (NI) REBCO double pancake (DP) coil were measured with the LFAC method. During the coil preparation, the upper pancake was loosened accidentally; thus, the upper and lower pancake coils had different turn-to-turn contact conditions. The experimental contact resistances were 631 μΩ for the upper pancake coil and 239 μΩ for the lower one, 937 μΩ for the whole. The simulation results well matched with the experimental values, showing 620 μΩ for the upper and 212 μΩ for the lower pancake coil. It was demonstrated that the LFAC method was able to measure the contact resistance of the NI DP coil even though it has different contact resistances on the upper and lower pancake coils.

The sudden discharge method was also applied. From the time constant of the decaying field, the experimentally obtained 971 μΩ showed good agreement with the LFAC method, while the simulated contact resistance was underestimated as 633 μΩ. The fair estimation with the simulation in the sudden discharge method remains as a future work.

From the simulation result of the sudden discharge, the lower pancake coil carries the current beyond the initial operating current. Also, the energy is consumed in the lower pancake twice as much as in the upper pancake during the sudden discharge.

Further analysis in the case of multi-stacked NI coils should be needed to investigate the thermal stability when the NI coils have different contact resistances.

References

[1] S. Hahn, D. K. Park, J. Bascuñán, and Y. Iwasa, "HTS Pancake Coils without Turn-to-Turn Insulation," *IEEE Trans. Appl. Supercond*., vol. 21, no. 3, pp. 1592–1595, 2011.

[2] S. Hahn et al., "45.5-Tesla Direct-Current Magnetic Field Generated with a High-Temperature Superconducting Magnet," *Nature*, vol. 570, no. 7762, pp. 496–499, 2019.

[3] D. Liu, D. Li, W. Zhang, H. Yong, and Y. Zhou, "Electromagnetic-Thermal-Mechanical Behaviors of a No-Insulation Double-Pancake Coil Induced by a Quench in The Self Field And The High Field," *Supercond. Sci. Technol.*, vol. 34, no. 2, 2021, Art. no. 025014.

[4] A. V. Gavrilin, D. J. Kolb-Bond, K. L. Kim, K. Kim, W. S. Marshall, and I. R. Dixon, "Quench and Stability Modelling of a Metal-Insulation Multi-Double-Pancake High-Temperature-Superconducting Coil," *IEEE Trans. Appl. Supercond*., vol. 31, no. 5, 2021, Art. no. 4601707.

[5] H. W. Weijers et al., "Progress in the Development of a Superconducting 32 T Magnet with REBCO High Field Coils," *IEEE Trans. Appl. Supercond.*, vol. 24, no. 3, 2014, Art. no. 4301805.

[6] K. Katsumata et al., "Influence of the Turn-to-Turn Contact Electrical Resistance on the Thermal Stability in Meter-Class No-Insulation REBCO Pancake Coils During a Local Normal-State Transition," *IEEE Trans. Appl. Supercond.*, vol. 27, no. 4, 2017, Art. no. 4602005.

[7] T. Mato and S. Noguchi, "Sudden Discharging and Overcurrent Simulations of REBCO Coils Coated with Conductive Epoxy Resin," *IEEE Trans. Appl. Supercond*., vol. 31, no. 5, 2021, Art. no. 4600705.

[8] D. Liu, W. Zhang, H. Yong, and Y. Zhou, "Thermal Stability and Mechanical Behavior in No-Insulation High-Temperature Superconducting Pancake Coils," *Supercond. Sci. Technol.*, vol. 31, no. 8, 2018, Art. no. 085010.

[9] X. Wang et al., "Turn-to-Turn Contact Characteristics for an Equivalent Circuit Model of No-Insulation ReBCO Pancake Coil," *Supercond. Sci. Technol*., vol. 26, no. 3, 2013, Art. no. 035012.

[10] S. Noguchi, R. Miyao, H. Okusa, T. Tatsuta, H. Ueda, and S. Kim, "Turn-to-turn Contact Resistance Measurement of No-Insulation REBCO Pancake Coils," *IEEE Trans. Appl. Supercond.*, vol. 29, no. 5, 2019, Art. no. 4601605.

[11] S. Noguchi, T. Tatsuta, D. Nishikawa, H. Ueda, and S. Kim, "Turn-to-turn Contact Resistance Measurement of No-Insulation REBCO Pancake Coil at DC Current Operation," *IEEE Trans. Appl. Supercond.*, vol. 30, no. 4, 2020, Art. no. 9000305.

[12] S. Noguchi et al., "Turn-to-Turn Contact Resistance Measurement of No-Insulation REBCO Pancake Coil: External Field Dependence," *IEEE Trans. Appl. Supercond*., vol. 31, no. 5, 2021, Art. no. 4602105.

[13] S. Kim, K. Miyamoto, H. Kobayashi, R. Inoue, H. Ueda, and S. Noguchi, "Experimental Study on the Accuracy of the Proposed LFAC Method for Measuring the Contact Resistance of NI HTS Coils," *IEEE Trans. Appl. Supercond*., vol. 32, no. 6, 2022, Art. no. 9001705.

[14] S. Kim et al., "Contact Resistance and Current Characteristics of NI HTS Coils in Low Frequency AC Method," *IEEE Trans. Appl. Supercond.*, vol. 33, no. 5, 2023, Art. no. 4601705.

[15] T. Mato, R. Inoue, H. Ueda, S. Kim, and S. Noguchi, "Investigation into Accuracy of Turn-To-Turn Contact Resistance Measurement in Low-Frequency AC Method by 3D Numerical Simulation," *Supercond. Sci. Technol*., vol. 36, no. 1, 2022, Art. no. 014005.

[16] S. Noguchi, "Electromagnetic, Thermal, and Mechanical Quench Simulation of NI REBCO Pancake Coils for High Magnetic Field Generation," *IEEE Trans. Appl. Supercond*., vol. 29, no. 5, 2019, Art. no. 4602607.

[17] G. Kim *et al.*, "Experimental Study and Frequency Domain Analysis on Metal-Insulation HTS Coil," *IEEE Trans. Appl. Supercond.*, vol. 32, no. 4, 2022, Art. no. 4600505.